Improvement of the WSR-88D Mesocyclone Algorithm

ROBERT R. LEE AND ANDERSON WHITE

WSR-88D Operational Support Facility, Norman, Oklahoma

(Manuscript received 19 March 1997, in final form 12 January 1998)

ABSTRACT

The build 9 Weather Surveillance Radar-1988/Doppler mesocyclone algorithm (B9MA) is designed to locate mesocyclones [rotating thunderstorm updrafts with diameters between 1.8 and 9.2 km (1–5 n mi)]. Because there is less than a one to one correspondence between tornadoes and mesocyclones, the B9MA alerts forecasters when it detects circulations that meet its criteria but tornadoes may not be observed. On the other hand, some tornadoes are not accompanied by large-scale meoscyclonic circulations. Weather radars cannot resolve small-scale tornadic circulations, and the B9MA may fail to alert forecasters that a tornado is present. The B9MA is only one of many tools that forecasters should use to predict tornado formation.

This paper describes limitations of the B9MA and how to improve its performance. The correlation between algorithmic detections and severe weather occurrence may be optimized under the premise that storms with strong, deep rotations are more likely to be associated with severe weather. Some tornadic circulations missed by the B9MA can be detected when the value of threshold pattern vector, a B9MA adaptable parameter, is lowered. When a rotational strength filter is added to the program logic, some algorithm detections of nontornadic mesocyclones can be eliminated.

1. Introduction

Storms containing strong, deep, rotating updrafts have a high likelihood of producing tornadoes, large hail (>2.0-cm diameter), and damaging wind (Fujita 1963); yet, based on a 20-yr study of Doppler radar data in Oklahoma, Burgess et al. (1993) observed only 30%–50% of supercell mesocyclones actually produce tornadoes. This dichotomy creates a dilemma both for the forecast meteorologist and for the programmer-meteorologist who designs and fine-tunes algorithms for the Weather Surveillance Radar-1988 Doppler (WSR-88D). The forecaster wants to be alerted to those mesocyclonic circulations potentially associated with tornadoes but at the same time cannot afford to be distracted by false alarms from the radar. In turn, the programmer must balance the radar software such that it detects most mesocyclonic circulations yet warns mainly on those with the potential for becoming severe.

The purposes of this paper are to explain some of the inner workings and limitations of the (current) build 9 WSR-88D mesocyclone algorithm (hereafter B9MA), to outline steps forecast offices may take to adjust the algorithm for optimum performance in their local warning areas, and to report on an integrated rotational strength (IRS) index, a potential improvement to mesocyclone evaluation by the WSR-88D.

The paper is organized as follows. There is a general discussion of mesocyclones and tornadoes that may or may not be detected by Doppler weather radar. Next, there is an explanation of how the B9MA processes data and a description of initial attempts to regionalize the algorithm through the use of adaptable parameters to minimize the number of false detections and reduce the bias toward Great Plains storms. This is followed by a historical perspective on operational rules of thumb pertaining to mesocyclone strength analysis coupled with recent strategies to incorporate these rules into calculating an IRS index. Results of several studies are presented. Finally, a summary and conclusions are offered along with suggestions for future research.

2. Limitations of detecting mesocyclones by Doppler weather radar

The first step forecasters can take toward improving B9MA performance is to consider several limitations: 1) The conceptual model is too simplistic, 2) all mesocyclones do not produce tornadoes, 3) radar geometry limits detection of smaller-scale rotational features, and 4) incorrectly dealiased Doppler velocities may cause misses or false alarms. Now we address each in turn.

Applying simplistic assumptions to complex, dynamic flow fields such as gust fronts and squall lines results in algorithm detections that alert forecasters to isolated, rotating updrafts and potentially severe circulations that

Corresponding author address: Dr. Robert R. Lee, NEXRAD Operational Support Facility, 1200 Westheimer Dr., Norman, OK 73069. E-mail: rlee@osf.noaa.gov

are not actually present. The B9MA examines Doppler velocity data, identifies regions of cyclonic shear, and models flow after a Rankine-combined vortex (Hennington and Burgess 1981; Wood and Brown 1983; Zrnić et al. 1985). Desrochers and Harris (1996) examined and questioned the assumptions inherent in the Rankine-combined vortex paradigm and developed a more sophisticated model. They proposed a nonsymmetrical flow model based on vorticity and divergence rather than on the Rankine-combined vortex design used as the basis of fielded WSR-88D software and National Severe Storms Laboratory (NSSL) developmental algorithms (Stumpf et al. 1998).

Since individual tornadic vorticies are too small to be identified by the B9MA except at very close range, forecasters should not expect the algorithm, in general, to detect nonsupercell tornadoes. Waterspouts and landspouts (associated with gust fronts, squall lines, hurricanes, derechos, and microbursts) are not usually accompanied by larger scale [1.8–9.2 km (1–5 n mi)] mesocyclonic circulations.

Radar limitations such as beam broadening, range–height dependency, and range folding work against a radar-based algorithm attempting to detect tornadic mesocyclones that form from small-scale, low-level rotations. Some F0, F1, and minisupercell tornadoes form within rotating thunderstorm updrafts that are shallow [less than 9.1 km (30 kft) deep] and small in diameter [less than 1.8 km (1 n mi)] (Burgess et al. 1995; Grant and Prentice 1996).

The WSR-88D velocity dealiasing algorithm determines velocity values for each data bin within the area of radar coverage. In regions of high shear, the dealiasing algorithm may assign erroneous or missing velocity values. Erroneous values have been known to cause the B9MA to generate false mesocyclone detections, and missing velocity values have caused circulations to be missed.

The B9MA alerts forecasters to storms that need no warning and fails, at times, to detect tornadic circulations. These limitations can be mitigated, to some degree, by fine-tuning algorithm adaptable parameters; however, the B9MA will never perform perfectly because there is much more to tornadogenesis than the presence of a mesocyclone. The next section outlines how the B9MA processes velocity data to locate mesocyclonic circulations and discusses initial attempts to optimize algorithm performance using adaptable parameters.

3. Algorithm design and adaptable parameters

The B9MA searches for cyclonic azimuthal shear patterns (pattern vectors) in Doppler velocity data that are partitioned into 0.25 km $\times$ 1° bins (Klazura and Imy 1993). Cyclonic shear is characterized by increasing radial velocity with increasing azimuth because the WSR-88D collects data in a clockwise manner. The search for the first pattern vector begins by comparing two velocity values from two adjacent bins at the same range from the radar. If cyclonic shear exists, Doppler velocity increases from the first bin to the second, and an ''open'' or incomplete pattern vector is created at the azimuth and range of the first velocity bin. The procedure continues for the next two radials, and so on, until cyclonic shear no longer is detected and the pattern vector is ''closed.'' In this manner, all pattern vectors within the radar volume scan are identified.

Momentum and shear values are calculated for each pattern vector as follows:

$$\text{Momentum} = |V_{\text{In}} - V_{\text{Out}}|(\text{Distance between } V_{\text{In}} \text{ and } V_{\text{Out}}), \quad (1)$$

and

$$\text{Shear} = \frac{|V_{\text{In}} - V_{\text{Out}}|}{\text{Distance between } V_{\text{In}} \text{ and } V_{\text{Out}}}, \quad (2)$$

where V_{In} and V_{Out} are maximum base velocity values toward and away from the radar, respectively (Zrnić et al. 1985). Momentum and shear values are compared to the following adaptable parameters: threshold high momentum (THM), threshold high shear (THS), threshold low momentum (TLM), and threshold low shear (TLS). A discussion of these parameters may be found in Zrnić et al. (1985) and Szoke (1988). The three-letter adaptable parameter designators are provided for WSR-88D operators so the names of the parameters contained in WSR-88D adaptable parameter menus can be correlated with their function. Pattern vectors that pass momentum and shear tests are expected to be characteristic of mesocyclones. Two-dimensional features are formed when a minimum number of pattern vectors [adaptable parameter threshold pattern vector (TPV)] are in close proximity to each other. Two-dimensional features are combined in the vertical to form three-dimensional features and mesocyclones are identified. For a full description of B9MA processing, see Tipton et al. (1998).

After the first WSR-88D radars were fielded at several locations around the country, forecasters noted the mesocyclone algorithm identified many circulations not associated with tornadoes. Since the mesocyclone algorithm was designed to detect velocity signatures with different size, strength, and shape characteristics, Operational Support Facility (OSF) personnel experimented with several case studies and raised threshold values of shear, momentum, and TPV to make the algorithm less sensitive. Algorithmic detections of nontornadic circulations decreased, but some tornadic mesocyclones, detected previously, were missed.

The WSR-88D has been fielded throughout the entire country and additional data have been collected. Forecasters note, when default adaptable parameter values are used in the B9MA, some tornadic mesocyclones are missed. The default adaptable parameters are based on research conducted in Oklahoma (Zrnić et al. 1985) and

TABLE 1. Mesocyclone adaptable parameters used to optimize performance.

Name	Mnemonic	Description	Low value	High value	Default value
Threshold high momentum ($km^2\ h^{-1}$)	THM	Min magnitude of angular momentum expected in a mesocyclone in the presence of low shear	180.0	1080.0	540.0
Threshold high shear (h^{-1})	THS	Min magnitude of shear expected in a mesocyclone in the presence of low angular momentum	7.2	28.8	14.4
Threshold low momentum ($km^2\ h^{-1}$)	TLM	Min magnitude of angular momentum in a mesocyclone	90.0	540.0	180.0
Threshold low shear (h^{-1})	TLS	Min magnitude of shear expected in a mesocyclone	3.6	14.4	7.2
Threshold pattern vector (dimensionless)	TPV	Min number of pattern vectors required to build a 2D feature	11	20	10

are shown in Table 1. Burgess et al. (1995) examined 18 cases from five different sites in the National Weather Service/Eastern Region and characterized minisupercell storms as having smaller rotational velocities, diminished horizontal diameters, and reduced vertical depths compared to their larger, stronger Great Plains counterparts. Algorithm developers conducted more experimental case studies, but this time, momentum, shear, and TPV adaptable parameter values were reduced to make the algorithm more sensitive to detect small-scale, slow-rotating thunderstorm updrafts. Initial attempts at improving the correlation between algorithm detections and severe weather produced mixed results. Additional tornadic mesocyclones were detected but the success was tempered by an increase in false alarms.

The experimental case studies highlighted the fact that algorithm developers could not decrease algorithm sensitivity to reduce the number of nontornadic mesocyclones detected and, at the same time, increase algorithm sensitivity to detect small-scale tornadic mesocyclones. This dichotomy was resolved by introducing another parameter: circulation strength.

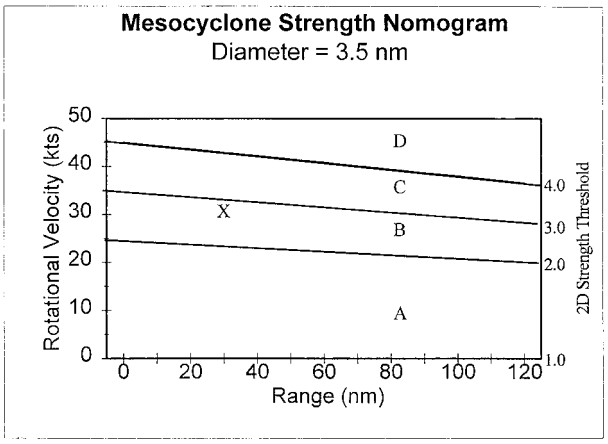

FIG. 1. Mesocyclone strength nomogram. Region A marks the weak shear region, region B marks the weak mesocyclone region, region C marks the moderate mesocyclone region, and region D marks the strong mesocyclone region. Each region of the graph is defined by 2D strength thresholds labeled 1.0, 2.0, 3.0, and 4.0 at the right. A circulation at a range of 30 n mi and a rotational velocity of 30 kt is classified by forecasters as a weak mesocyclone, has a 2D strength threshold of approximately 2.8, and is marked by label X. IRS Strength (a 3D strength value) is calculated by adding all of the 2D strength thresholds of each 2D slice contained in a 3D circulation.

4. Mesocyclone rotational strength

Operational use of rotational velocity to classify mesocyclone strength evolved from Joint Doppler Operational Project (JDOP) field studies conducted during the mid 1970s (JDOP Staff 1979). NSSL scientists modified Donaldson's mesocyclone recognition criteria (Burgess 1976) to use azimuthal shear and maxima in inbound/outbound radial velocities (JDOP Staff 1979). Shear thresholds were replaced by rotational velocity during the Doppler/lightning '87 exercise (Forsyth et al. 1989). Researchers at NSSL continued to study rotational velocity in several statistical studies, such as Burgess (1976) and Burgess et al. (1982). Forecasters at the National Weather Service Forecast Office (NWSFO) in Norman experimented with rotational velocity as an important parameter soon after the initial WSR-88D radars were installed.

Andra (1997) describes how rotational velocity thresholds were established in the early 1990s for severe thunderstorm and tornado warning guidance. Relationships among radar beamwidth, rotational velocity, circulation size, range, and mesocyclone strength thresholds were combined in the WSR-88D mesocyclone recognition nomogram shown in Fig. 1. The nomogram displays qualitative mesocyclone strength for a circulation of radius 6.5 km (3.5 n mi), given the range on the *x* axis and the observed rotational velocity (derived from maxima in inbound/outbound radial velocities) on the *y* axis. Lines of mesocyclone strength 1) slope downward with increasing range, 2) slope more with range for diameters on the order of 1.8 km (1 nm) and less with range for diameters on the order of 9.3 km (5 nm), and 3) divide the graph into four regions: weak shear, weak mesocyclone, moderate mesocyclone, and strong mesocyclone. (Figure 1 is explained in more detail in section 5.)

In the mid-1990s, radar/warning meteorologists in the United States manually evaluated measurements of observed rotational velocity and range using the nomogram in Fig. 1 and assessed mesocyclone strength for tornado warning guidance. Nomogram strength thresh-

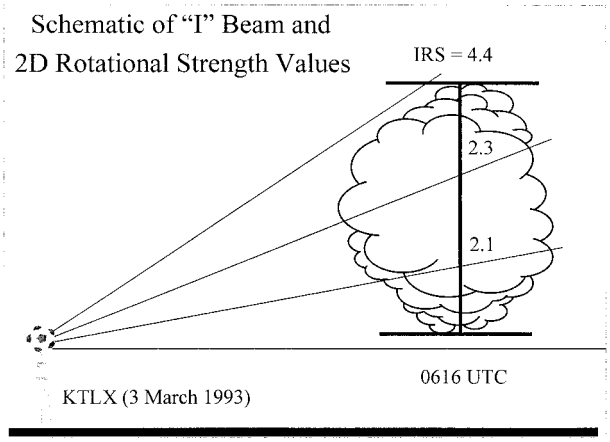

FIG. 2. A schematic illustrating an I beam defining the base and top of a storm. The 2D rotational strength values, calculated from the mesocyclone strength nomogram, are plotted along the side of the I where the radar beam intersects the storm. The IRS index, shown above the I, is obtained by adding the 2D rotational strength values. This illustration is from a tornadic storm observed from Oklahoma City (KTLX) at 0616 UTC 3 March 1993.

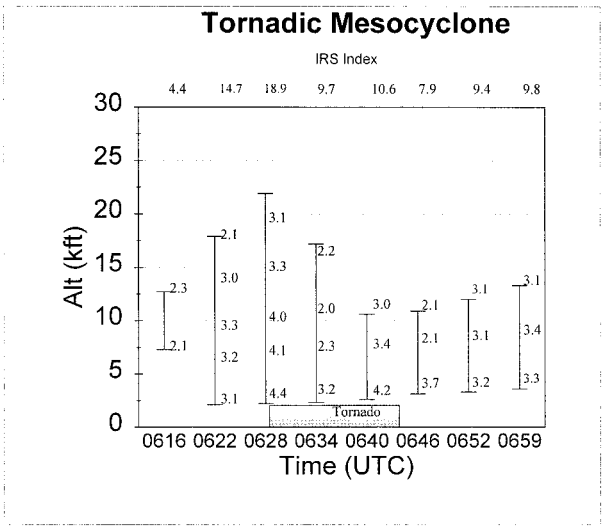

FIG. 3. The bases, tops, and depths of 3D features are represented by I Beams along a time line on the *x* axis for an Oklahoma tornado that occurred on 30 March 1993. Each slice of each 3D circulation is labeled with a 2D strength value to the right of each I Beam. IRS values are calculated by adding up the 2D strength values in the vertical along each I Beam and are displayed across the top of the graph.

olds were based on Oklahoma supercells and may not have represented other weather phenomena, environments, or climatological regimes. As a result, operational forecasters outside the Great Plains adjusted their thresholds accordingly. Recognizing algorithm and radar limitations, forecasters used the mesocyclone recognition nomograms to help decide which circulations merited a warning.

5. Strategy for improving the Build 9 mesocyclone algorithm

a. Development of the integrated rotational strength index

Donaldson and Desrochers (1990) and Desrochers (1991) anticipated tornado forecasting by mesocyclone detection alone would yield a high false alarm rate because one half or less of all mesocyclones are tornadic (Burgess and Lemon 1990). Donaldson and Desrochers investigated a variable known as excess rotational kinetic energy (ERKE). This variable was defined as the rotational kinetic energy in excess of that necessary to maintain mesocyclonic shear, defined mathematically and confirmed observationally as 0.005 s^{-1} (Donaldson 1970). ERKE was shown to be effective in predicting strong to violent tornadoes but less effective in predicting weaker circulations producing only minimal ground damage. Only a few high plains supercells were examined.

In 1995, WSR-88D OSF algorithm developers chose not to use ERKE but implemented a similar concept building on the mesocyclone recognition nomogram technique already in use by operational forecasters. A dimensionless, two-dimensional (2D) strength index, with values beginning with 1.0, is shown as the right ordinate in Fig. 1. An index value is assigned to each 2D feature of the mesocyclonic circulation intersected by the radar beam. For example, point X in Fig. 1 represents a 2D feature with diameter 6.4 km (3.5 n mi), range 55.5 km (30 n mi), rotational velocity 15.4 m s^{-1} (30 kt), and rotational strength index approximately 2.8, a weak mesocyclone. The numerically modeled nomogram uses radar-observed mesocyclone diameters rather than the fixed, average diameter 6.4 km (3.5 n mi) used in the manual nomogram. Lines that divide the nomogram into separate regions are steeper for mesocyclones with diameters less than 6.4 km (3.5 n mi) and shallower for mesocyclones with diameters greater than 6.4 km (3.5 n mi).

Strength values of each 2D slice of the mesocyclone are added together to obtain an IRS index as shown in Fig. 2. The IRS index is calculated by summing all 2D rotational strength indices from circulation base to top. If the B9MA identifies more than one 2D feature at a particular elevation angle in proximity to other 2D features, only the strongest 2D feature is included in the integrated strength value.

Figure 3 shows a series of IRS indices constructed to give a time sequence of mesocyclone development during which a tornado was observed. The IRS index values from each volume scan are displayed above the associated 2D mesocyclone summary. The corresponding UTC time is shown as the abcissa. Note the tornado appeared when the IRS index was at a maximum and persisted through the next two volume scans.

How should forecasters use this index, and what value distinguishes tornadic from nontornadic mesocyclonic

TABLE 2. Contingency table used to calculate algorithm performance.

	Observed yes	Observed no
Forecast yes	The number of B9MA detections associated with tornadic circulations that have IRS values greater than or equal to some critical value	The number of B9MA detections that have IRS values greater than or equal to the critical value but are not associated with tornadic circulations
Forecast no	The number of B9MA detections associated with tornadic circulations that have IRS values less than some critical value plus the number of tornadic circulations that B9MA failed to identify	N/A

circulations? The IRS indices displayed along the top of Fig. 3 range from 4.4 to 18.9. Algorithm developers examined many circulations in several case studies described below and found no single, critical, IRS value correctly identified all tornadic mesocyclones yet yielded no false alarms. Therefore, the critical IRS value was made adaptable. Increasing the critical IRS value causes the B9MA to mark only the strongest circulations, and lowering the value below one causes the B9MA to label all circulations. Critical IRS values were determined for each case study by repeatedly running and scoring the algorithm using a range of IRS values and then selecting the value that maximized the critical success index (CSI) (Doswell et al. 1990). Critical IRS values ranged between five and seven, depending on the dataset examined.

b. Algorithm scoring and testing the IRS index: Case studies 1 and 2

Witt et al. (1998) developed procedures to evaluate radar algorithm performance. Radar data are examined and compared to tornado and wind damage reports from *Storm Data* (NCDC 1992–94) to determine locations and times of damage-causing storms. Severe storms are followed backward in time four volume scans from the point of reported damage to define the beginning of a time window. The end of a time window is defined one volume scan after the damage report. Algorithm developers identify circulations associated with damage-causing storms within each time window. These manually truthed circulations become the ground truth against which algorithm detections are compared. Table 2 shows a contingency table with the rules used to count algorithm hits, misses, and false alarms from which algorithm performance measures [probability of detection (POD), false alarm ratio (FAR), and CSI] are calculated (Doswell et al. 1990).

In study 1, B9MA performance was calculated using manually truthed level II data collected from the Oklahoma City radar (KTLX) on 11 May 1992. Algorithm developers computed algorithm performance statistics for a range of IRS values from 0.1 to 8.0. Figure 4 shows the effectiveness of the IRS index in reducing the number of false alarms. The lowest critical IRS value of 0.1 allows all detections to be counted, just as if the IRS filter had not been applied because the critical value is below the smallest possible IRS value of 1.0. As the IRS critical value increases, the FAR decreases. Eventually, the POD is affected and begins to drop as well. The CSI is at a maximum when the IRS index has a value of seven. (See label A in Fig. 4.)

A set of eight data cases, comprising 33.5 h, 336 volume scans, and 611 circulation identifications, was used to develop and fine-tune IRS calculations in study 2 as summarized in Table 3. The storms, selected primarily because they were the most complete data cases that had been collected at that time, were isolated supercell events. Default adaptable parameters, listed in Table 1, were used and IRS values were calculated.

Detections from the B9MA were compared with manually truthed circulations. Algorithm developers calculated performance statistics for a range of IRS values from two to eight. In study 2, an IRS value of six maximized performance scores. CSI values for study 2, with and without the IRS index, are shown in Fig. 5. Over the eight cases, use of the IRS index reduced the number false alarms, resulting in a CSI increase of 10%, on average.

Both the mesocyclone strength nomogram in use at NWSFOs and the IRS index use rotational velocity to rank circulation strength. The first two studies show the number of nontornadic detections can be decreased by applying the IRS filter. The decrease probably occurs because storms associated with strong, deep rotations are more likely to be associated with severe weather.

Early work characterizing mesocyclones was conducted in the Great Plains and few small circulations were originally studied. Since then, data collected by the WSR-88D network revealed mini-supercells and other very small tornadic circulations. The next two studies concentrated on increasing algorithm sensitivity. As more smaller circulations are detected, the IRS index can be applied to help distinguish tornadic from nontornadic circulations.

c. Changing algorithm adaptable parameters: Case studies 3 and 4

Researchers from the OSF Applications Branch tuned the B9MA to detect smaller-scale circulations by reducing the value of TPV, the adaptable parameter that represents the minimum number of pattern vectors required to build a 2D feature. In study 3, archive level

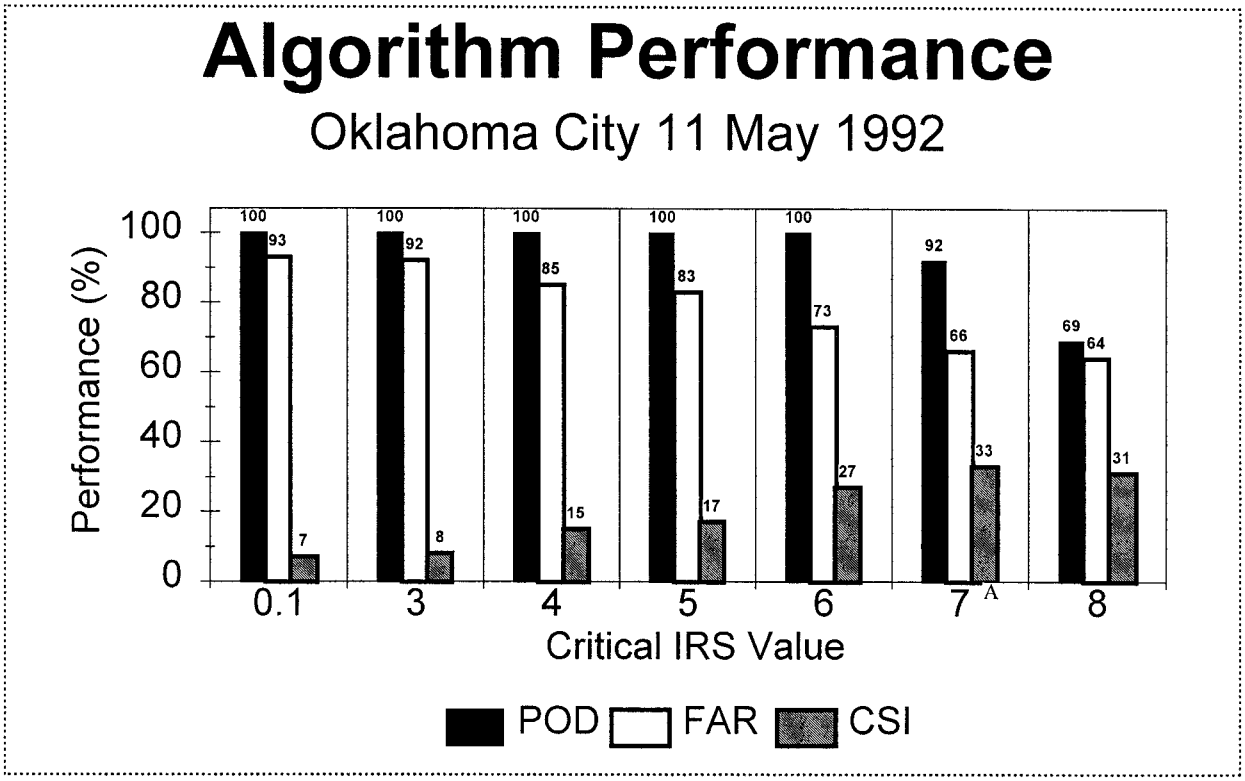

FIG. 4. Study 1. Algorithm performance for Oklahoma City 11 May 1992 as a function of critical IRS value. The first bar in each series plots POD, the second bar depicts FAR, and the third bar shows CSI. Label A shows algorithm performance optimized with a critical IRS value of 7.

II data from six minisupercell tornadoes were manually truthed and algorithm performance was calculated using TPV values of 10, the default value, and 6. (A TPV value of 3 was also tested; however, values below 6 taxed the processing capabilities of the current WSR-88D hardware.) Table 4 lists times and locations of the minisupercell tornadoes and Fig. 6 shows results from study 3. The POD for tornado detection increases significantly as the value of TPV is decreased without increasing the FAR. Reducing TPV from 10 to 6 improved B9MA performance on the six minisupercells studied.

Szoke (1988) showed, of the 15 adaptable parameters used by the B9MA, momentum and shear thresholds were most useful in modifying algorithm performance.

TABLE 3. Study 2. Eight cases included in the preliminary algorithm improvement study.

Case	City	Date
1	Oklahoma City, OK	11 May 1992
2	Oklahoma City, OK	3 Mar 1993
3	Dodge City, KS	7 May 1993
4	Houston, TX	16 Nov 1994
5	Melbourne, FL	28 May 1992
6	Sterling, VA	27 Jul 1994
7	Melbourne, FL	13 Mar 1993
8	Des Moines, IA	15 Apr 1994

Beginning with default settings, adaptable parameter values for momentum, shear, and pattern vector number were lowered systematically to increase algorithm sensitivity. Fifteen adaptable parameter sets were tested in study 4 (Table 5). In general, algorithm sensitivity increased from parameter set A through O.

In study 4, OSF algorithm developers tuned the B9MA to generate more detections and relied on the IRS index to separate tornadic from nontornadic circulations. Four days and 289 volume scans of level II data selected for analysis are summarized in Table 6. Output from the B9MA was filtered by IRS index and verified against manually truthed circulations from tornado reports rather than both tornado and wind reports used in previous case studies. The B9MA detected many (10 816) circulations during the study period when adaptable parameter thresholds were lowered to make the algorithm more sensitive.

As in study 2, OSF algorithm developers calculated performance statistics for a range of IRS values from 2 to 8. An IRS value of 5 maximized algorithm performance. Performance scores were calculated for each adaptable parameter set listed in Table 5 and are presented in subsequent figures.

Figure 7 shows algorithm performance statistics from Dodge City, Kansas, 5 May 1993, one day from the data

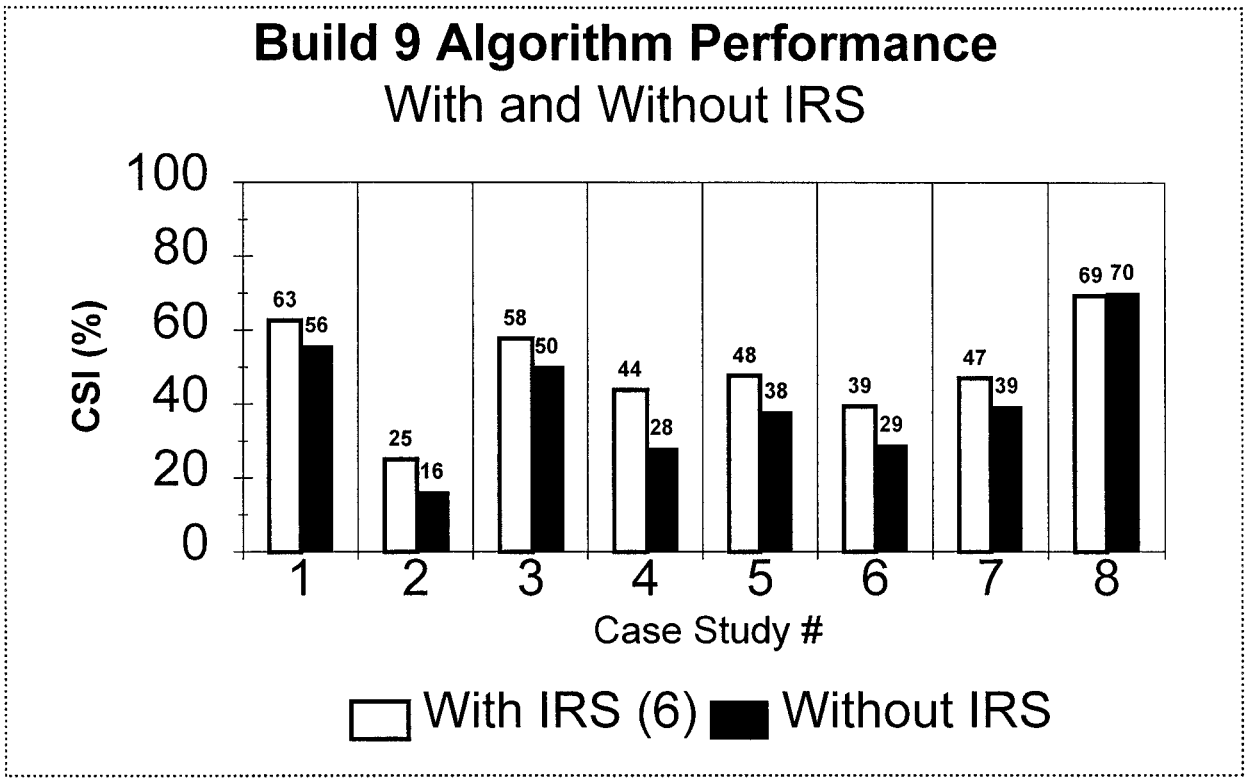

FIG. 5. Study 2. The first bar in each series plots the CSI algorithm performance for each case study day using an IRS value of 6. The second bar depicts CSI values without using the IRS index to filter out false alarms.

used in study 4. As parameter threshold values were lowered, POD increased and open bars became taller graphically, illustrating the B9MA detected more circulations than when the default adaptable parameter values were used. False alarms, low for set A, increased and remained at nearly the same level for sets B–H, J, and K. False alarms were higher for set I and increased rapidly in sets L–O. CSI was a maximum in parameter set H.

All algorithm detections from all days in study 4 were combined. CSI values, calculated for each adaptable parameter set, are shown in Fig. 8. Algorithm performance using the IRS filter was the same or higher than the performance not using the filter. When the algorithm was adjusted to detect more circulations and the IRS filter was applied, CSI improved. As in Fig. 7, adaptable parameter set H maximized performance.

TABLE 4. Study 3. Times and locations of six minisupercell tornadoes (Torn.).

Date (1993)	Local time (EST)	Event	County	State
16 Apr	1925	F0 Torn.	Loudoun	VA
16 Apr	2035	F1 Torn.	Loudoun	VA
16 Apr	2100	F0 Torn.	Fauquier	VA
16 Apr	0730	F1 Torn.	Fauquier	VA
16 Apr	1500	F1 Torn.	Queen Annes	MD
26 Apr	0900	F1 Torn.	Warren	VA

Figure 8 also shows algorithm performance without IRS filtering. Of the parameter sets studied, set B optimized CSI. The B9MA performed better in both study 3 and study 4 when the number of pattern vectors required to make a 2D feature, TPV, was lowered from 10 to 6.

Figure 9 compares algorithm performance between the default adaptable parameter set and the optimized adaptable parameter set H with IRS filtering for each day of study 4. The CSI increase was higher on some

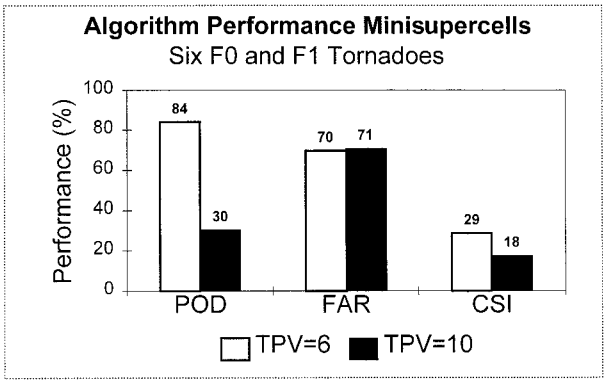

FIG. 6. Study 3. Mesocyclone algorithm performance values (POD, FAR, CSI) are plotted along the ordinate for six minisupercell tornadoes that occurred in the northeast United States in 1993.

TABLE 5. Study 4. Fifteen adaptable parameter sets developed for algorithm optimization. (See Table 1 for definitions of TPV, THS, THM, TLS, and TLM.)

Param. set	TPV	THS (h^{-1})	THM ($km^2\ h^{-1}$)	TLS (h^{-1})	TLM ($km^2\ h^{-1}$)
A	10	14.4	540	7.2	180
B	6	14.4	540	7.2	180
C	3	14.4	540	7.2	180
D	10	14.4	540	3.6	90
E	6	14.4	540	3.6	90
F	3	14.4	540	3.6	90
G	10	7.2	540	7.2	180
H	6	7.2	540	7.2	180
I	6	7.2	540	3.6	90
J	10	7.2	180	7.2	180
K	10	7.2	180	3.6	90
L	6	7.2	180	3.6	90
M	3	7.2	180	3.6	90
N	3	7.2	540	3.6	90
O	6	7.2	540	3.6	90

days than on others, but the performance increase was most pronounced for a minisupercell case from Sterling, Virginia, on 30 April 1994. (This minisupercell case is different from the minisupercell cases examined in study 3, documented in Table 4.)

TABLE 6. Study 4. Four cases included in the second independent algorithm improvement study.

Case	City	Date
1	Sterling, VA	30 Apr 1994
2	Oklahoma City, OK	17 Sep 1994
3	Tulsa, OK	6 May 1994
4	Dodge City, KS	5 May 1993

d. Primary results

To achieve the best possible performance with the B9MA, only two adaptable parameters need to be modified from their default values: 1) if the IRS index is applied to reduce false alarms, the THS value should be lowered from 14.4 h^{-1} to 7.2 h^{-1} and the TPV value should be lowered from 10 to 6, and 2) if the IRS index is not applied, the TPV value should be lowered from 10 to 6. Both of these actions appear to improve B9MA performance over the default, baseline configuration. Algorithm improvements using the IRS filter or some other equivalent cannot be implemented until WSR-88D software is updated sometime in the future; however, forecasters can lower the TPV adaptable parameter value to improve B9MA performance now.

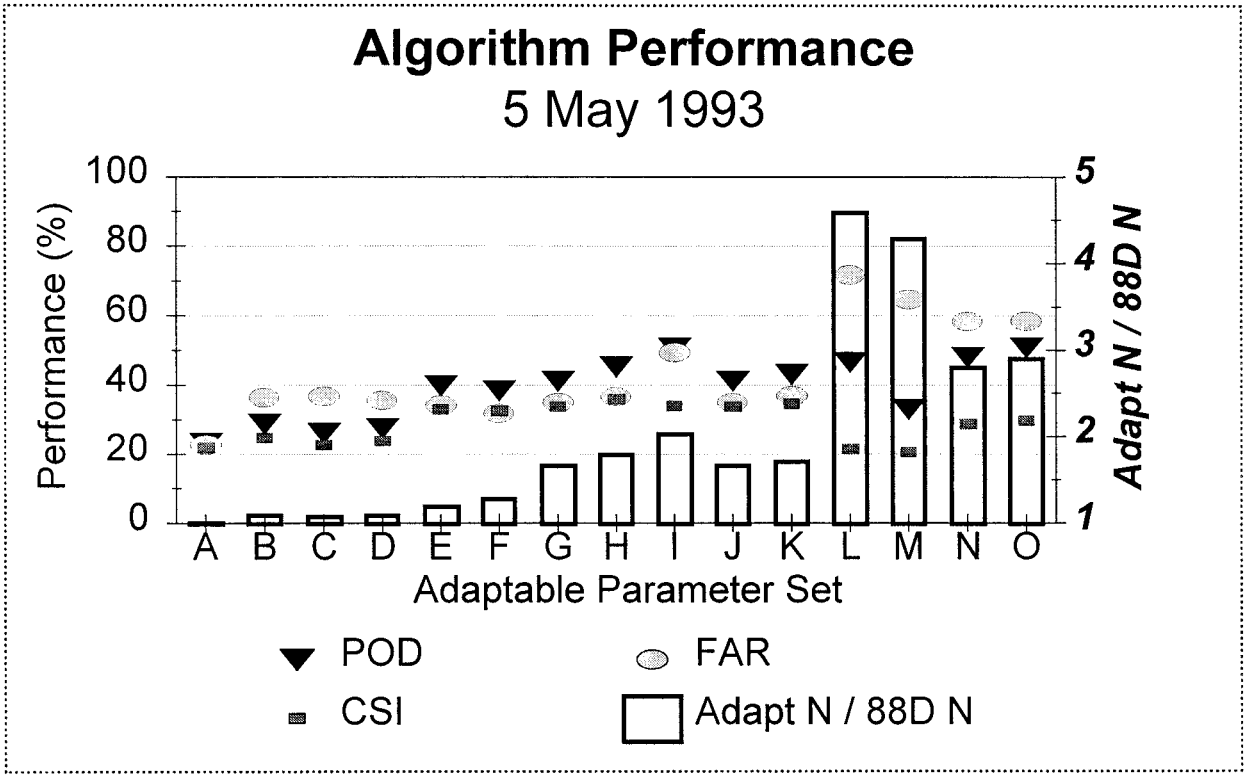

FIG. 7. Study 4, 1 day. Algorithm performance from three tornadoes—F0, F1, F4, 5 May 1993, Dodge City, KS. POD, triangular markers; FAR, oval markers; and CSI, square markers are shown for each adaptable parameter set A–O. The open bars, Adapt N/88D N, scale to right, represent the number of circulations detected using a given adaptable parameter set divided by the number of circulations detected when the default parameter set, A, was used. This ratio represents the additional number of detections processed as the algorithm located weaker and smaller-scale circulations.

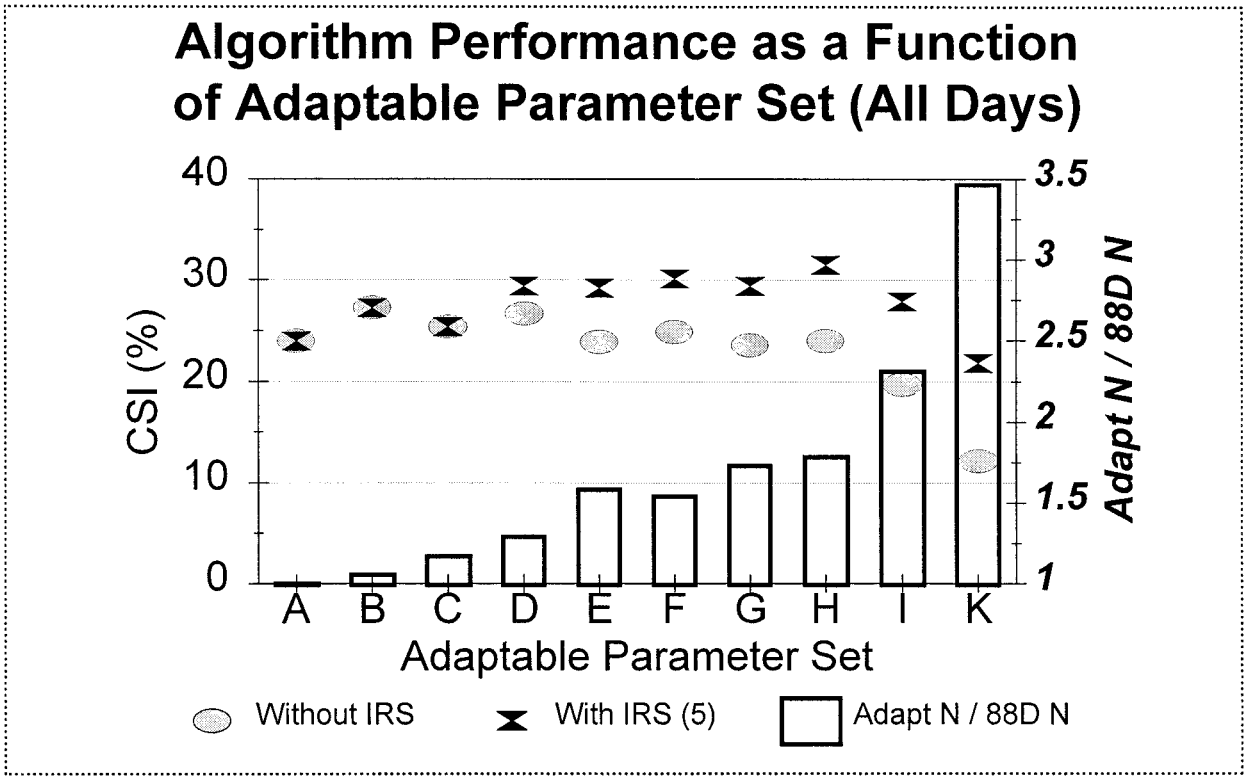

FIG. 8. Study 4, all days. Filled ovals represent CSI values without IRS filtering and hourglass markers represent algorithm performance using an IRS value of 5. The open bars depict the same function as in Fig. 7, but the values are different here because Figure 7 represents algorithm performance from only one day from study 4 and here all days from study 4 are represented.

Forecasters at WSR-88D radar sites across the country have been notified that lowering the TPV adaptable parameter value enables the B9MA to detect previously missed smaller scale mesocyclones and have been cautioned that the number of false alarms might increase. The algorithm already finds many nontornadic mesocyclones, and the IRS index has not been fielded to reduce the number of nontornadic detections. Anecdotal evidence from forecasters at Minneapolis, Minnesota; Jackson, Mississippi; Sterling, Virginia; Melbourne, Florida; Portland, Oregon; and other sites confirms reducing the TPV value increases the algorithm's overall performance at the expense of additional false alarms for low-topped supercells.

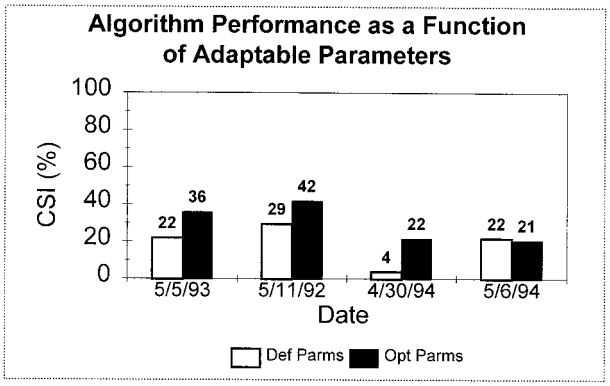

FIG. 9. Study 4. The first bar in each series displays algorithm CSI performance using default adaptable parameter set A. The second bar displays the algorithm CSI using optimized adaptable parameter set H (lower value of THS, lower value of TPV, and IRS filtering).

6. Summary and conclusions

The build 9 mesocyclone algorithm is designed to detect mesocyclones. If a mesocyclone is detected, then the accompanying storm has a higher likelihood of producing severe weather, but tornado formation is not guaranteed. No matter how well algorithm performance is optimized, there will always be mesocyclones without severe weather, tornadoes without mesocyclones, tornadoes associated with weak mesocyclones, and mesocyclones with tornadoes too far away from the radar to be detected. The correlation between B9MA detections and tornadoes can be increased by classifying circulation strength via the IRS index [to decrease false alarms and optimize adaptable parameters to increase the number of tornadic mesocyclone detections].

NWSFOs around the country have been authorized to modify the TPV adaptable parameter value based on the findings described in this paper. Some forecast office

personnel are conducting parameter studies in an attempt to optimize B9MA for their own regions. Many offices report that reducing the TPV parameter value from its default setting to a value between 10 and 6 improves B9MA performance.

7. Future research

The high cost associated with fielding new algorithms is mitigated by improving B9MA performance with adaptable parameter adjustments. Next-generation algorithms are being designed to evaluate a spectrum of severe weather phenomena. Algorithm design details such as liberal acceptance of pattern vectors; more robust rules used to link 1D, 2D, and 3D features; rule bases; and neural networks to classify circulations are being investigated (Marzban and Stumpf 1995, 1996; Stumpf et al. 1998). An entirely new paradigm is being researched (Trafalis et al. 1997; Jeyabalan et al. 1998) in which neural networks are applied directly to WSR-88D base data (reflectivity, velocity, and spectrum width) to locate tornadic mesocyclones using pattern matching techniques.

An important limitation of the B9MA is that a single conceptual model is applied to many different types of convective activity, such as isolated supercells, minisupercells, comma heads of bow echoes, hurricane rainbands, and leading edges of squall lines. Better understanding of tornado formation mechanisms and conceptual models are also needed.

In the future, automated circulation classification likely will provide better estimates of storm severity. Forecasters will continue to assess storm and mesocyclone circulation strengths, and enhanced algorithms will provide improved guidance with longer lead times. We anticipate forecasters will have more time to evaluate other aspects of severe storms including environment, storm reflectivity structure, and spectrum width. In addition to being informed the algorithm has found a circulation, forecasters will benefit from knowledge about rotational strength and likelihood that the storm is, or may become, severe.

Acknowledgments. The authors thank Don Burgess for his helpful insight and Tim O'Bannon for valuable discussions about the WSR-88D source code. Thanks also go to Greg Stumpf and other NSSL staff who provided insight into mesocyclone analysis and detection problems and potential solutions.

REFERENCES

Andra, D. L., 1997: The origin and evolution of the WSR-88D mesocyclone recognition nomogram. Preprints, *28th Conf. on Radar Meteorology,* Austin, TX, Amer. Meteor. Soc., 364–365.

Burgess, D. W., 1976: Single Doppler radar vortex recognition: Part I: Mesocyclone signatures. Preprints, *17th Conf. on Radar Meteorology,* Seattle, WA, Amer. Meteor. Soc., 97–103.

——, and L. R. Lemon, 1990: Severe thunderstorm detection by radar. *Radar in Meteorology,* D. Atlas, Ed., Amer. Meteor. Soc., 619–647.

——, V. T. Wood, and R. A. Brown, 1982: Mesocyclone evolution statistics. Preprints, *12th Conf. on Severe Local Storms,* San Antonio, TX, Amer. Meteor. Soc., 422–424.

——, R. J. Donaldson, and P. R. Desrochers, 1993: Tornado detection and warning by radar. *The Tornado: Its Structure, Dynamics, Predictions and Hazards, Geophys. Monogr.,* No. 79, Amer. Geophys. Union, 203–221.

——, R. R. Lee, S. S. Parker, D. L. Floyd, and D. L. Andra Jr., 1995: A study of minisupercells observed by WSR-88D radars. Preprints, *27th Conf. on Radar Meteorology,* Vale, CO, Amer. Meteor. Soc., 4–6.

Desrochers, P. R., 1991: Automatic mesocyclone detection and tornado forecasting. PL-TR-912051, Phillips Laboratory, Hanscom Air Force Base, MA, 168 pp. [Available from Phillips Laboratory, Air Force Systems Command, Hanscom Air Force Base, MA 01731-3010.]

——, and F. I. Harris, 1996: Interpretation of mesocyclone vorticity and divergence structure from single-Doppler radar. *J. Appl. Meteor.,* **35,** 2191–2209.

Donaldson, R. J., 1970: Vortex signature recognition by a Doppler radar. *J. Appl. Meteor.,* **9,** 661–670.

——, and P. R. Desrochers, 1990: Improvement of tornado warnings by Doppler radar measurement of mesocyclone rotational kinetic energy. *Wea. Forecasting,* **5,** 247–258.

Doswell, C. A., III, R. Davies-Jones, and D. L. Keller, 1990: On summary measures of skill in rare event forecasting based on contingency tables. *Wea. Forecasting,* **5,** 576–585.

Forsyth, D. E., D. W. Burgess, L. E. Mooney, M. H. Jain, C. A. Doswell III, D. W. Rust, and R. E. Rabin, 1989: DOPLIGHT 87 program summary. NOAA Tech. Memo. ERL NSSL-101, National Severe Storms Laboratory, Norman, OK, 183 pp.

Fujita, T., 1963: Analytical mesometeorology: A review. *Severe Local Storms, Meteor. Monogr.,* No. 27, Amer. Meteor. Soc., 77–125.

Grant, B., and R. Prentice, 1996: Mesocyclone characteristics of minisupercell thunderstorms. Preprints, *15th Conf. on Weather and Forecasting,* Norfolk, VA, Amer. Meteor. Soc., 362–365.

Hennington, L. D., and D. W. Burgess, 1981: Automatic recognition of mesocyclones from single Doppler radar data. Preprints, *20th Conf. on Radar Meteorology,* Boston, MA, Amer. Meteor. Soc., 704–706.

JDOP Staff, 1979: Final report of the joint Doppler operational project. NOAA Tech. Memo. ERL NSSL-86, National Severe Storms Laboratory, Norman, OK, 84 pp.

Jeyabalan, C., A. White, and T. Trafalis, 1998: Statistical analysis of base data from the WSR-88D weather radar and description of mesocyclone features using neural networks. Preprints, *14th Conf. on Probability and Statistics in the Atmospheric Sciences,* Phoenix, AZ, Amer. Meteor. Soc., J93–J96.

Klazura, G. E., and D. A. Imy, 1993: A description of the initial set of analysis products available from the NEXRAD WSR-88D system. *Bull. Amer. Meteor. Soc.,* **74,** 1293–1311.

Marzban, C., and G. J. Stumpf, 1995: A neural network for the diagnosis of tornadic and severe-weather yielding storm-scale circulations. Preprints, *27th Conf. on Radar Meteorology,* Vail, CO, Amer. Meteor. Soc., 224–226.

——, and ——, 1996: A neural network for tornado prediction based on Doppler radar-derived attributes. *J. Appl. Meteor.,* **35,** 617–626.

National Climatic Data Center (NCDC), 1992–1994: *Storm Data.* Vols. 34–36.

Stumpf, G. J., A. Witt, E. D. Mitchell, P. L. Spencer, J. T. Johnson, M. D. Eilts, K. W. Thomas, and D. W. Burgess, 1998: The National Severe Storms Laboratory Mesocyclone Detection Algorithm for the WSR-88D. *Wea. Forecasting,* **13,** 304–326.

Szoke, E., 1988: A summary of NEXRAD activities at PROFS. NOAA, Boulder, CO, 90 pp. [Available from NOAA/ERL/FSL/PROFS, Boulder, CO 80303.]

Tipton, G. A., E. D. Howieson, J. M. Margraf, and R. R. Lee, 1998: Optimizing the WSR-88D Mesocyclone/Tornadic Vortex Signature Algorithm using WATADS—A case study. *Wea. Forecasting,* **13,** 367–376.

Trafalis, T. B., N. P. Covellan, P. Li, G. Stumpf, and A. White, 1997: An affine scaling neural network training algorithm for prediction of tornadoes. *Artificial Neural Networks in Industrial Engineering (ANNIE '97),* Rolla, MO, University of Missouri.

Witt, A., M. D. Eilts, G. J. Stumpf, E. D. Mitchell, J. T. Johnson, and K. W. Thomas, 1998: Evaluating the performance of WSR-88D severe storm detection algorithms. *Wea. and Forecasting,* **13,** 513–518.

Wood, V. T., and R. A. Brown, 1983: Single Doppler velocity signatures: An atlas of patterns in clear air/widespread precipitation and convective storms. NOAA Tech. Memo. ERL NSSL-95, 71 pp. [NTIS PB84155779.]

Zrnić, D. S., D. W. Burgess, and L. D. Hennington, 1985: Automatic detection of mesocyclonic shear with Doppler Radar. *J. Atmos. Oceanic Technol.,* **4,** 425–438.